Journal of Chromatography A, 1452 (2016) 107–115

Contents lists available at ScienceDirect

Journal of Chromatography A

journal homepage: www.elsevier.com/locate/chroma

Molar mass fractionation in aqueous two-phase polymer solutions of dextran and poly(ethylene glycol)

Ziliang Zhao[a,c], Qi Li[a,d], Xiangling Ji[a], Rumiana Dimova[b], Reinhard Lipowsky[b], Yonggang Liu[a,b,*]

[a] State Key Laboratory of Polymer Physics and Chemistry, Changchun Institute of Applied Chemistry, Chinese Academy of Sciences, 130022 Changchun, China
[b] Department of Theory and Bio-Systems, Max Planck Institute of Colloids and Interfaces, Science Park Golm, 14424 Potsdam, Germany
[c] University of Chinese Academy of Sciences, 100049 Beijing, China
[d] School of Chemical Engineering, Changchun University of Technology, 130012 Changchun, China

ARTICLE INFO

Article history:
Received 19 January 2016
Received in revised form 7 April 2016
Accepted 27 April 2016
Available online 28 April 2016

Keywords:
Aqueous two-phase system
Dextran
Poly(ethylene glycol)
GPC
Fractionation
Partition

ABSTRACT

Dextran and poly(ethylene glycol) (PEG) in phase separated aqueous two-phase systems (ATPSs) of these two polymers, with a broad molar mass distribution for dextran and a narrow molar mass distribution for PEG, were separated and quantified by gel permeation chromatography (GPC). Tie lines constructed by GPC method are in excellent agreement with those established by the previously reported approach based on density measurements of the phases. The fractionation of dextran during phase separation of ATPS leads to the redistribution of dextran of different chain lengths between the two phases. The degree of fractionation for dextran decays exponentially as a function of chain length. The average separation parameters, for both dextran and PEG, show a crossover from mean field behavior to Ising model behavior, as the critical point is approached.

1. Introduction

Polymeric aqueous two-phase systems (ATPSs) can be formed by mixing aqueous solutions of two different polymers, such as dextran and poly(ethylene glycol) (PEG), above a certain concentration. Two immiscible phases largely containing water are obtained, with one phase rich in dextran and the other one rich in PEG. Such ATPSs are widely employed for the separation and purification of proteins, nucleic acids, viruses and cells [1,2], due to their biocompatibility and the unique feature to provide a mild environment with extremely low interfacial tension. ATPSs can be employed in microfluidic setups [3], as well as in large scales [4], for the separation and purification of biological materials. The partitioning of biomolecules or cells in ATPS is not only controlled by their own physico-chemical affinities to the two phases or the liquid-liquid interface, but also influenced by the properties of the ATPS such as the tie line length and the molar mass of polymers, etc [5–7]. The interfacial tension between the coexisting phases, which depends on the composition and molar mass of polymers in the phases, also plays an important role in the partitioning of cells in ATPS [8]. It is therefore important to study the phase behaviors of ATPS and find their correlations with the partitioning of specific samples.

Accurate determination of the tie lines of dextran-PEG system is not trivial. To measure the polymer concentrations in each phase, usually one has to measure two physical properties, such as optical rotation and refractive index, of both phases [9]. The dextran concentration in the phase is determined by a polarimeter, while the PEG concentration is obtained after subtracting the dextran contribution to the refractive index. A gravimetric method was introduced to determine the tie lines of ATPS containing PEG and salt, by measuring the weight of two coexisting phases and forcing the tie line end points on a predetermined binodal fitted with an empirical equation [10]. One must be careful to apply this method for the dextran-PEG system considering the polydispersity of generally available dextran, because the tie line end points do not exactly match the binodal of ATPS for polymers with broad molar mass distributions. Recently, we introduced a simple density method to determine the tie lines of the dextran–PEG system by measuring the density of the coexisting phases [11]. The approach was

* Corresponding author at: State Key Laboratory of Polymer Physics and Chemistry, Changchun Institute of Applied Chemistry, Chinese Academy of Sciences, 130022 Changchun, China.
E-mail addresses: yonggang@ciac.ac.cn, Yonggang.Liu@mpikg.mpg.de (Y. Liu).

http://dx.doi.org/10.1016/j.chroma.2016.04.075
0021-9673/

based on the assumption that end points of the tie lines lie on the binodal, which is a good approximation when polymers with narrow molar mass distributions are employed. Phase separation in polydisperse polymer solutions has been considered both theoretically and experimentally [12–18]. It has been shown that during phase separation of aqueous mixtures of dextran with either gelatin or poly(ethylene oxide), all having broad molar mass distributions, fractionation of both species occurs [19,20]. While in ATPSs containing dextran with a broad molar mass distribution and PEG with a narrow molar mass distribution, the molar mass of dextran in the dextran-rich phase is much larger than that in the PEG-rich phase, and no significant molar mass difference of PEG in the two phases is found [21,22]. A number of different theoretical models for phase equilibria of ATPS have been reported in the literature [23,24], such as the model based on osmotic viral expansions [25,26], the lattice model based on Flory-Huggins theory [27] and the UNIQUAC model [18,28]. An effective excluded volume model has also been developed using methods of statistical geometry for the calculation of the binodal curves of ATPS [29]. Zaslavsky et al. proposed that phase separation in ATPS is due to the incompatibility of the polymer-modified water structures [30]. These models describe the experimental phase diagram reasonably well, but a comprehensive theory is still lacking. Additionally, the coexisting phases of ATPS offer distinct physical and chemical environments which allow for the selective partitioning of solutes such as proteins. Protein partitioning in ATPS is related to the polymer concentration difference between the phases via parameters such as the molar mass of polymers, protein-polymer interaction parameters, and the electrostatic potential difference between the phases [31,32]. Very recently, it was shown that the protein partitioning in ATPS is governed by the solvatochromic solvent properties of the coexisting phases [33,34], which depends on the composition and molar mass of the phase-forming polymers. Therefore, studying the phase diagram and molar mass fractionation of the dextran-PEG system, not only contributes to a better understanding of the liquid-liquid equilibria in ATPS, but also provides new insights into the mechanisms of biomolecules partitioning in ATPS.

In the present study, we performed gel permeation chromatography (GPC) measurements on the coexisting phases of the aqueous mixtures of dextran and PEG. Tie lines were constructed based on the GPC data and compared with a previous method based on density measurements of the phases. Molar mass fractionation of dextran and PEG during phase separation was studied and compared with theory.

2. Material and methods

2.1. Materials

Dextran from the bacterium Leuconostoc mesenteroides (molar mass between 400 and 500 kg/mol, lot number BCBG1982V) and PEG (molar mass 8 kg/mol, lot number MKBD4398V) were purchased from Sigma-Aldrich; they were desiccated in vacuum until no further reduction in mass was observed before use. All other reagents were of analytical grade. All solutions were prepared using ultrapure water from Sartorius water purification system with a resistivity of 18.2 MΩ cm.

2.2. Phase separation

Cloud-point titration was employed to determine the binodal and the critical point of dextran and PEG aqueous solution at 25 ± 1 °C [11]. Concentrated stock solutions of dextran and PEG (10–20% by weight) were prepared by dissolving polymers in water. To establish the binodal curve, a certain concentration of dextran (or PEG) solution was prepared by adding water to the dextran (or PEG) stock solution in a 10 mL vial. Then PEG (or dextran) stock solution was added dropwise into the vial followed by shaking. The titration was continued until the solution became turbid. The mass of each stock solution and water was measured by a balance to establish the binodal curve. The critical point, at which the phase volumes are equal as one approaches the binodal from the two-phase region, was determined by titration as described elsewhere [11]. To construct the tie lines, mixtures of dextran and PEG solutions were prepared in the two-phase region in 50 mL separating funnels by keeping the weight ratio between dextran and PEG equal to that at the critical point. The solutions were shaken by hand to ensure good mixing of the polymers. The samples were kept at a temperature of 25 ± 1 °C for one week to ensure complete phase separation before the PEG-rich phase was taken from the upper outlet and the dextran-rich phase was collected from the lower one. The density of each separated phase was measured at 25 ± 0.01 °C by a density meter (DMA4500, Anton Paar) with a resolution of 5×10^{-5} g/mL.

2.3. Gel permeation chromatography

GPC measurements were performed on separated phases to obtain both composition and molar mass distribution of dextran and PEG in each phase [22]. The GPC system was equipped with two PL aquagel-OH mixed-H columns (7.5 × 300 mm, Polymer Laboratories Ltd.) and a 2414 differential refractive index (RI) detector (Waters Corporation). The eluent of water containing 0.02 wt% NaN_3 was delivered by a Waters 515 HPLC pump at a constant flow rate of 1.0 mL/min. The separated phases were diluted 10–100 times with the eluent and 100 μL polymer solution was injected to the system via a Waters 717plus autosampler. The concentration of dextran and PEG in each separated phase was obtained from the area of the eluting peaks for dextran and PEG using calibration curves relating the RI peak area to the injected polymer concentration. The molar mass of dextran and PEG in each separated phase was determined after calibrating the columns with narrow PEG and poly(ethylene oxide) (PEO) standards obtained from Polymer Laboratories Ltd. Universal calibration was applied to obtain the molar mass of dextran [35–37], which was validated by coupling GPC with a DAWN HELLEOS II multi-angle laser light scattering detector (Wyatt Technology Corporation).

3. Results and discussion

3.1. Binodal and critical point

The binodal of the aqueous solution of dextran and PEG is shown in Fig. 1. It should be noted that for data points with large weight fraction of PEG ($w_p > 0.06$), the weight fraction of dextran is very small with $w_d < 0.001$. Even a small amount of high molar mass dextran is immiscible with a concentrated PEG solution, due to the unfavorable interaction between the long dextran chains and the PEG molecules. Following the protocol in Ref. [11], a series of polymer solutions in the two-phase region at a certain weight ratio w_d/w_p between dextran and PEG were prepared, and the volume fraction of each phase was measured when gradually approaching the binodal by adding water. The volume fraction Φ^D of the dextran-rich phase in the vicinity of the phase boundary is plotted as a function of w_d/w_p in the inset of Fig. 1. The volumes of the dextran-rich and PEG-rich phases are equal ($\Phi^D = 0.50$) at the weight ratio $w_d/w_p = 1.23$. Carefully studying the phase behavior of solutions close to the binodal with w_d/w_p fixed at 1.23 gave the composition of the critical point of the system with a total polymer weight fraction of $w_{cr} = 0.0811 \pm 0.0002$. The phase dia-

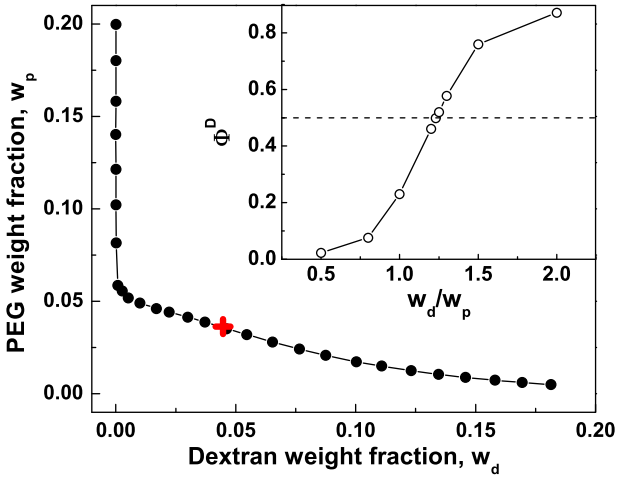

Fig. 1. Binodal of aqueous solution of dextran and PEG at 25 °C obtained by titration (solid circles). The "+" symbol indicates the composition of the critical point ($w_{d,cr}$ = 0.0447, $w_{p,cr}$ = 0.0364). The upper inset shows the dependence of the volume fraction Φ^D of the dextran-rich phase on the weight ratio w_d/w_p in the vicinity of the binodal. For Φ^D = 0.50 (dashed line), the polymer weight ratio w_d/w_p = 1.23.

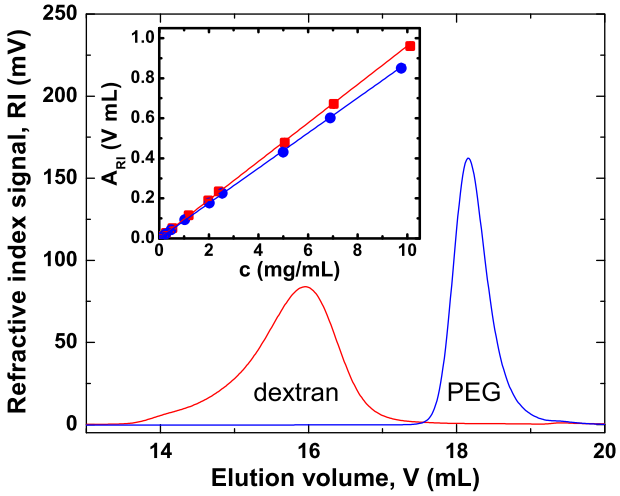

Fig. 2. GPC chromatograms for dextran with injected concentration of 1.18 mg/mL (red curve) and PEG with injected concentration of 1.02 mg/mL (blue curve). Dextran is eluted earlier with a peak retention volume of 16.0 mL, while PEG is eluted later with a peak retention volume of 18.2 mL. The inset shows the dependence of the RI peak area A_{RI} as a function of the polymer mass density or concentration c of the solutions injected into the GPC columns for dextran (red squares) and PEG (blue circles). The straight lines are linear fits to the data with $A_{RI} = kc$ where k = 0.09613 for dextran and k = 0.08774 for PEG, respectively. (For interpretation of the references to colour in this figure legend, the reader is referred to the web version of this article.)

gram differs slightly compared to previous results [11], due to both batch-to-batch differences in the molar mass distribution of the polymers from the same manufacturer [38] and the subtle difference in temperature. Phase separation of ATPS was performed at 25 ± 1 °C in the present study, which was slightly different from 24 ± 0.5 °C in Ref. [11]. However, one should keep in mind that the phase diagram of ATPS containing dextran and PEG is sensitive to the temperature [38]. We performed GPC measurements for dextran and PEG in the present study, as well as for those samples in Ref. [11]. We found that the molar mass distribution of PEG is nearly the same in both studies. However, dextran used in the present study has a weight average molar mass M_w = 380 kg/mol and a number average molar mass M_n = 174 kg/mol (see further below), compared to M_w = 487 kg/mol and M_n = 174 kg/mol for the polymer used in Ref. [11]. Our conclusion is that one should always determine the phase diagram of ATPS when new lots of polymer samples are used.

3.2. Locating the tie lines by GPC measurements

The compositions of the separated phases in the ATPS system of dextran and PEG solutions were determined by GPC with a RI detector. Fig. 2 shows the typical chromatograms for dextran and PEG with injected concentration of about 1 mg/mL. It can be seen that dextran is eluted earlier from the GPC columns than PEG, due to the fact that the studied dextran molecules are much larger than the PEG molecules. We then integrated the RI peaks individually and plotted the RI peak area A_{RI} as a function of injected polymer concentration c, from which we obtained the calibration curves; see the inset of Fig. 2. Linear relations were established for both dextran and PEG solutions over a broad range of concentration between 0.1 and 10 mg/mL.

In the next step, each separated phase was diluted and analyzed by GPC. Fig. 3 shows the GPC chromatograms of three couples of the coexisting dextran-rich and PEG-rich phases with different initial polymer weight fractions of (w_d, w_p) = (0.0452, 0.0367), (0.0534, 0.0434), and (0.1606, 0.1306), respectively. One can easily identify the peaks of dextran and PEG from each chromatogram, because baseline separations of the two components were achieved. From the RI peak height and area, it is obvious that with increasing polymer concentration, more dextran is partitioned into the dextran-rich phase, and more PEG is distributed into the PEG-rich phase. At the highest polymer concentrations, no PEG is found in the

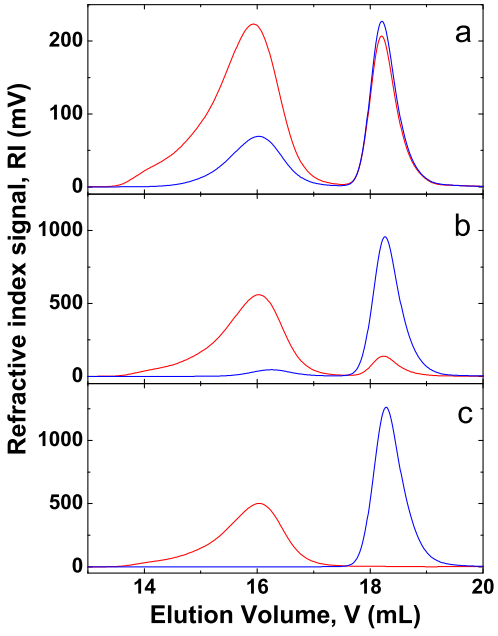

Fig. 3. GPC chromatograms of coexisting dextran-rich (red curve) and PEG-rich (blue curve) phases. The panels (a)-(c) correspond to initial polymer weight fractions of (w_d, w_p) = (0.0452, 0.0367), (0.0534, 0.0434), and (0.1606, 0.1306), respectively. (For interpretation of the references to colour in this figure legend, the reader is referred to the web version of this article.)

dextran-rich phase and no dextran is found in the PEG-rich phase. The polymer concentrations in each of the phases were calculated from the peak areas of dextran and PEG using the calibration curves in Fig. 2. The polymer weight fractions in the dextran-rich phase, (w_d^D, w_p^D) and those in the PEG-rich phase, (w_d^P, w_p^P), i.e., the end points of the respective tie line, were then obtained with the known dilution ratio before each GPC measurement. Table 1 summarized the resulting compositions of dextran-rich and PEG-rich phases obtained by the GPC method, which had a typical coefficient of variation of about 1%.

Table 1
Compositions of dextran-rich and PEG-rich phases obtained by the GPC method.

ε	w_d	w_p	Dextran-rich phase				PEG-rich phase				Δw
			w_d^D	w_p^D	ρ^D (g/mL)	$\rho^{D,cal}$ (g/mL)[a]	w_d^P	w_p^P	ρ^P (g/mL)	$\rho^{P,cal}$ (g/mL)[a]	
0.0098	0.0452	0.0367	0.0659	0.0269	1.02805	1.02757	0.0255	0.0452	1.01464	1.01456	0.00038
0.030	0.0461	0.0374	0.0745	0.0242	1.03099	1.03058	0.0189	0.0490	1.01276	1.01261	0.00046
0.092	0.0487	0.0396	0.0931	0.0188	1.03793	1.03727	0.0099	0.0568	1.01045	1.01039	0.00051
0.134	0.0506	0.0411	0.1033	0.0165	1.04162	1.04109	0.0070	0.0604	1.00993	1.00985	0.00050
0.200	0.0534	0.0434	0.1157	0.0139	1.04660	1.04581	0.0043	0.0656	1.00973	1.00969	0.00052
0.302	0.0579	0.0470	0.1332	0.0108	1.05362	1.05262	0.0021	0.0727	1.01004	1.01003	0.00058
0.389	0.0616	0.0501	0.1465	0.0090	1.05887	1.05801	0.0012	0.0786	1.01061	1.01067	0.00036
0.508	0.0667	0.0542	0.1639	0.0071	1.06551	1.06517	0.0006	0.0854	1.01162	1.01158	0.00044
0.599	0.0706	0.0574	0.1756	0.0060	1.07035	1.07011	0.0004	0.0909	1.01249	1.01244	0.00042
0.729	0.0761	0.0618	0.1907	0.0048	1.07700	1.07655	0.0001	0.0989	1.01372	1.01371	0.00037
0.982	0.0867	0.0705	0.2173	0.0033	1.08883	1.08824	0.0000	0.1141	1.01630	1.01625	0.00048
1.552	0.1102	0.0896	0.2684	0.0017	1.11287	1.11166	0.0000	0.1486	1.02234	1.02220	0.00116
2.087	0.1317	0.1071	0.3162	0.0000	1.13518	1.13447	0.0000	0.1806	1.02808	1.02778	0.00152
2.825	0.1606	0.1306	0.3760	0.0000	1.16434	1.16486	0.0000	0.2255	1.03627	1.03573	0.00121
3.605	0.1901	0.1546	0.4347	0.0000	1.19651	1.19629	0.0000	0.2730	1.04490	1.04427	0.00082

[a] The densities of dextran-rich phases $\rho^{D,cal}$ and those of PEG-rich phases $\rho^{P,cal}$ were calculated according to $\rho = [(1 - w_d - w_p)\nu_s + w_d\nu_d + w_p\nu_p]^{-1}$ with the specific volume of water ν_s = 1.00297 mL/g, the specific volume of dextran ν_d = 0.61871 mL/g and that of PEG ν_p = 0.83680 mL/g, which were measured by the density meter at 25 °C.

The tie lines were established by the GPC method over a broad range of polymer concentrations, which were characterized by the normalized distance to the critical point

$$\varepsilon \equiv c/c_{cr} - 1 \quad (1)$$

where the critical concentration c_{cr} = 0.0828 ± 0.0002 g/mL. Fig. 4 shows the tie lines established by the GPC method when the reduced concentration ε was varied between 0.01 and 3.6. The accuracy of the tie lines is supported by the fact that the initial composition of the polymer solutions (indicated by "+" symbols in Fig. 4), lie close to the corresponding tie line, with an averaged distance Δw between the initial composition and the tie line of less than 0.0007 (Table 1).

We also measured the density of each separated phase by a density meter and established the tie lines as described previously [11], and the tie lines found from both methods agreed very well. A typical example is shown in Fig. 4 for the initial composition (w_d, w_p) = (0.0867, 0.0705). The measured densities of the two phases are ρ^D = 1.08883 g/mL for the dextran-rich phase and ρ^P = 1.01630 for the PEG-rich phase. The intersections of the isopycnic lines with the binodal yield the composition of the dextran-rich phase (w_d^D, w_p^D) = (0.2188, 0.0028) and that of the PEG-rich phase (w_d^P, w_p^P) = (0.0000, 0.1144). These values are very close to those obtained by the GPC method (see Table 1): (w_d^D, w_p^D) = (0.2173, 0.0033) and (w_d^P, w_p^P) = (0.0000, 0.1141). The averaged difference of the phase compositions obtained by the GPC and density methods for all compositions is about 0.001, showing good agreement. This conclusion was also supported by the fact that the calculated densities of the polymer phases according to their composition obtained by the GPC method coincided well with the measured densities (with an averaged difference of 3×10^{-4} g/mL, see Table 1). The density method is relatively simple and requires only the densities of the co-existing phases to be measured, with the binodal established by titration. Even though the GPC method is more complex and time-consuming, it is independent of the binodal curve. In addition, the GPC method can provide details about the molar mass distribution of each polymer species in the separated phases, as we will show below. One caveat is that the GPC method with RI detection is only applicable to ATPSs with a large size difference between the two polymers. If these two polymers have similar sizes and are eluted at about the same time from the GPC columns, one needs two concentration detectors, such as a RI and an optical rotation detector [19,20], to determine the concentration of each polymer component. The end points of the tie lines agree well with the binodal curve, except for the data points of the PEG-rich phases close to the critical point with $0.01 < \varepsilon < 0.2$, which is probably due to polydispersity of dextran (we will come back to this point in the next sections).

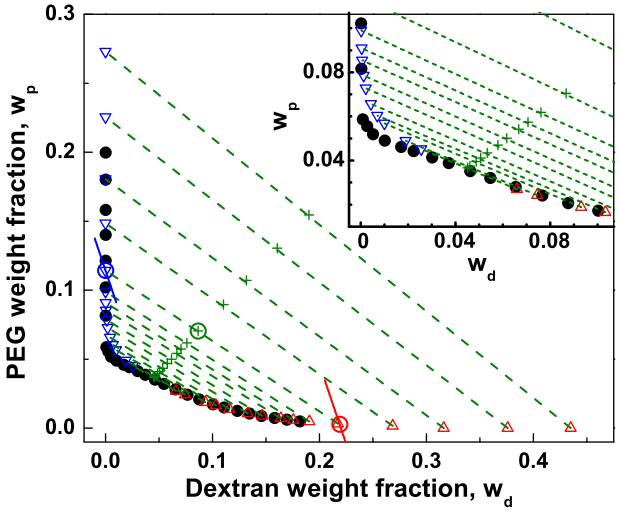

Fig. 4. Tie lines in the dextran—PEG phase diagram. The solid circles represent the experimentally measured points of the binodal (same data as in Fig. 1). The compositions of the initial solutions (with weight ratio w_d/w_p = 1.23), for which GPC measurements after phase separation were performed, are indicated by "+" symbols. The end points of the respective tie lines are shown with upward-pointing triangles indicating the compositions of the dextran-rich phases and downward-pointing triangles indicating the compositions of the PEG-rich phases. The solid lines show two examples of the isopycnic lines for the initial composition indicated with an encircled "+" symbol in the graph: (w_d, w_p) = (0.0867, 0.0705). The compositions of the two phases obtained from the intersections of the isopycnic lines with the binodal are shown as open circles. The inset shows the enlarged region of the phase diagram close to the critical point.

From the compositions corresponding to the tie line end points as established by the GPC method, we calculate the order parameter of the coexisting phases, i.e., the composition difference Δc corresponding to the length of the tie line expressed by polymer mass concentration. This composition difference and the density difference $\Delta\rho$ are plotted as functions of the reduced polymer concentration ε in Fig. 5. The effective scaling exponent β in $\Delta\rho \sim \varepsilon^{\beta}$ and $\Delta c \sim \varepsilon^{\beta}$ depends on the distance from the critical point, as previously observed by the density method [11]: (i) in the concentration range $0.01 < \varepsilon < 0.14$ (regime I), we observed 0.342 ± 0.017 as estimated from the density difference dependence and 0.348 ± 0.017 as estimated from the composition

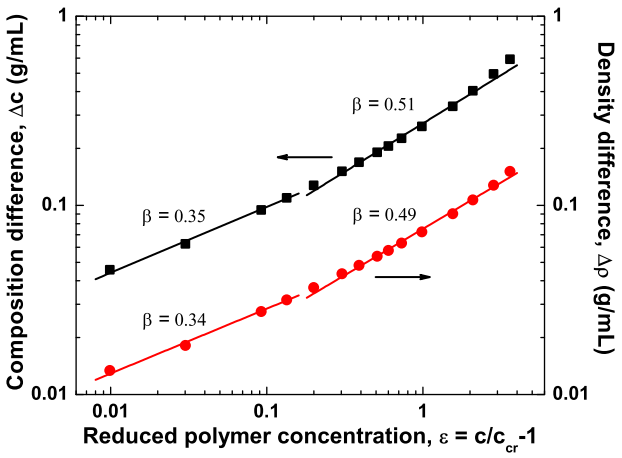

Fig. 5. Composition difference Δc (solid squares) and density difference $\Delta\rho$ (solid circles) of the coexisting phases as functions of the reduced polymer concentration ε. In the concentration range $0.01 < \varepsilon < 0.14$, the effective scaling exponent β has the value 0.342 ± 0.017 as estimated from the density difference and 0.348 ± 0.017 as estimated from the composition difference, while in the range $0.2 < \varepsilon < 3$, we obtained exponent values 0.490 ± 0.012 from the density difference and 0.511 ± 0.013 from the composition difference.

difference dependence, and (ii) in the range $0.2 < \varepsilon < 3$ (regime II), we obtained 0.490 ± 0.012 from the density difference dependence and 0.511 ± 0.013 from the composition difference dependence. These values are in good agreement with the Ising value of $\beta = 0.326$ for regime I and the mean field value $\beta = 1/2$ for regime II.

3.3. Molar mass distribution of dextran and PEG in ATPS

Apart from measuring the polymer concentration, the GPC measurement can also provide the molar mass distributions of each component in the separated phases. Inspection of Fig. 3 shows that the elution peak of dextran in the PEG-rich phase is not only smaller in height than that in the dextran-rich phase, but also shifts towards the higher retention volume, corresponding to a lower molar mass. The difference between the dextran elution peaks in the two phases grows with the distance from the critical point. At the same time, the elution peak of PEG is hardly changed in retention volume for the two phases at all initial polymer concentrations, although the peak height in the dextran-rich phase is smaller than that in the PEG-rich phase. This indicates that the molar mass distribution of PEG between the two phases does not change but only the total amount does.

The precise molar mass distributions of dextran and PEG in both phases were obtained from the calibration curves relating the molar mass of each polymer with the retention volume. The results for dextran and PEG are summarized in Table 2 and Table 3, respectively. Fig. 6 shows an example at initial polymer concentration $(w_d, w_p) = (0.0452, 0.0367)$, or reduced polymer concentration $\varepsilon = 0.01$. The original dextran has a broad molar mass distribution with $M_w = 380$ kg/mol, $M_n = 174$ kg/mol, and a polydispersity index $M_w/M_n = 2.19$ (Table 2). For dextran in the dextran-rich phase we obtained $M_w = 454$ kg/mol, $M_n = 193$ kg/mol, and $M_w/M_n = 2.35$, while $M_w = 249$ kg/mol, $M_n = 153$ kg/mol, and $M_w/M_n = 1.63$ were found for dextran in the PEG-rich phase. This is because the high molar mass component of dextran was enriched in the dextran-rich phase and depleted from the PEG-rich phase (Fig. 6a). As the initial polymer concentration increases, the molar mass of dextran in the dextran-rich phase decreases towards that of the original sample, while the M_w of dextran in the PEG-rich phase continuously decreases to 82.2 kg/mol at $\varepsilon = 0.73$, see Fig. 7 and Table 2. At higher polymer concentration with $\varepsilon > 0.73$, the amount of dextran in the PEG-rich phase is so small that it can hardly be detected by GPC. On

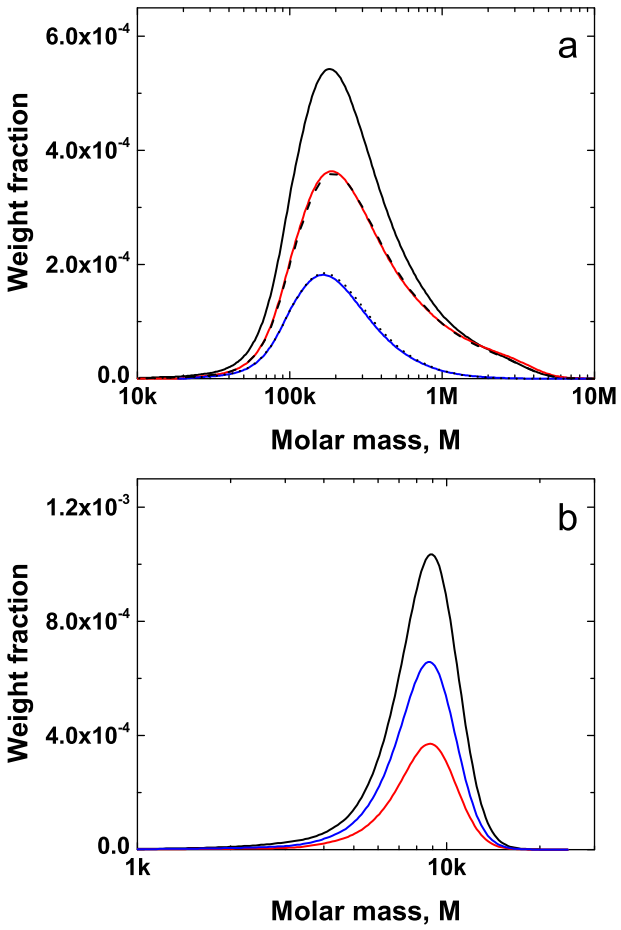

Fig. 6. Measured molar mass distribution of dextran (a) and PEG (b) in the initial polymer (black curve), dextran-rich phase (red curve) and PEG-rich phase (blue curve) at reduced polymer concentration $\varepsilon = 0.01$. The calculated molar mass distribution of dextran in the two phases are also shown as dashed and short dashed lines in panel (a). (For interpretation of the references to colour in this figure legend, the reader is referred to the web version of this article.)

the other hand, the original PEG has a narrow molar mass distribution with $M_w = 8.45$ kg/mol, $M_n = 7.64$ kg/mol, and $M_w/M_n = 1.11$ (Table 3). The molar mass distributions of PEG in the two coexisting phases are almost the same (Fig. 6b). An increase of the initial polymer concentration does not lead to significant change of the molar mass and the molar mass distribution of PEG in the two phases (Fig. 7 and Table 3). It should be noted that in Fig. 6, the area under each molar mass distribution curve is proportional to the weight fraction of each polymer component in the initial and the co-existing phases of the polymer solutions. The summations of the molar mass distribution of dextran and PEG in the two phases agree very well with the molar mass distribution of the original samples (Fig. 6). It indicates that the GPC method provides accurate results for the concentration and the molar mass distribution of each component in ATPSs. The molar mass distributions of dextran in the two phases were also calculated from (i) the dependence of the degree of fractionation of dextran on its molar mass (Fig. 8) and (ii) the weight fraction of the phases, which were in excellent agreement with the GPC measurements (Fig. 6a). In the next section, we will discuss the fractionation of dextran and PEG based on their molar mass distribution in the two coexisting phases.

3.4. Molar mass fractionation of dextran and PEG in ATPS

Consider all chains of one polymer component, x, with a certain chain length as characterized by the number N of monomers. The

Table 2
Molar mass averages of dextran in dextran-rich and PEG-rich phases.

ε	Dextran-rich phase			PEG-rich phase		
	M_w (kg/mol)	M_n (kg/mol)	M_w/M_n	M_w (kg/mol)	M_n (kg/mol)	M_w/M_n
native	380.0	173.7	2.19	380.0	173.7	2.19
0.0098	453.9	192.9	2.35	249.3	152.6	1.63
0.030	426.9	182.0	2.35	208.9	138.3	1.51
0.092	394.1	172.1	2.29	167.6	120.8	1.39
0.134	397.9	177.8	2.24	152.3	112.5	1.35
0.200	380.6	170.3	2.23	136.0	103.1	1.32
0.302	369.8	164.2	2.25	116.9	90.0	1.30
0.389	373.3	167.1	2.23	109.4	84.8	1.29
0.508	371.3	164.6	2.26	97.1	76.9	1.26
0.599	370.6	163.1	2.27	95.9	69.4	1.38
0.729	375.2	166.0	2.26	82.2	66.9	1.23
0.982	372.4	163.7	2.28			
1.552	368.7	161.8	2.28			
2.087	368.6	155.8	2.37			
2.825	374.7	160.5	2.34			
3.605	368.7	161.8	2.28			

Table 3
Molar mass averages of PEG in dextran-rich and PEG-rich phases.

ε	Dextran-rich phase			PEG-rich phase		
	M_w (kg/mol)	M_n (kg/mol)	M_w/M_n	M_w (kg/mol)	M_n (kg/mol)	M_w/M_n
native	8.45	7.64	1.11	8.45	7.64	1.11
0.0098	8.38	7.57	1.11	8.35	7.58	1.10
0.030	8.12	7.33	1.11	8.35	7.61	1.10
0.092	8.08	7.25	1.11	8.30	7.52	1.10
0.134	8.18	7.31	1.12	8.41	7.65	1.10
0.200	8.02	7.06	1.14	8.39	7.63	1.10
0.302	8.02	7.00	1.15	8.28	7.53	1.10
0.389	7.98	6.89	1.16	8.40	7.63	1.10
0.508	7.93	6.69	1.19	8.38	7.60	1.10
0.599	7.88	6.55	1.20	8.50	7.70	1.10
0.729	7.78	6.22	1.25	8.29	7.49	1.11
0.982				8.44	7.65	1.10
1.552				8.63	7.82	1.10
2.087				8.43	7.64	1.10
2.825				8.40	7.57	1.11
3.605				8.56	7.76	1.10

partitioning of these chains between the two phases is described by the degree of fractionation (or the distribution coefficient) $f_x(N)$. According to Flory-Huggins theory, this quantity behaves as [27]

$$f_x(N) = c_{x,poor}(N)/c_{x,rich}(N) = exp(-\sigma_x N) \quad (2)$$

where $c_{x,poor}(N)$ and $c_{x,rich}(N)$ are the mass densities of polymer component x (here dextran or PEG) with chain length N in the x-poor and x-rich phases, respectively. Thus, according to this theory, the degree of fractionation $f_x(N)$ should decay exponentially with increasing chain length N, i.e., the long x-chains are almost exclusively in the x-rich phase. The separation parameter σ_x, according to the complex expression provided by the Flory-Huggins theory [17,27], depends on temperature, pressure, and polymer concentration. This parameter represents the free energy change per monomer involved in transferring a chain of length N from one phase to the other [27]. The present study was conducted at temperature of 25 °C and standard atmosphere.

In Fig. 8, we plot the degree of fractionation for dextran $f_d(N)$ as a function of dextran chain length N_d for different values of the reduced polymer concentration ε. An exponential dependence on the chain length N is indeed observed over a certain range of N-values which depends on the value of ε, although the curves are slightly concave. According to computer simulations, the deviation of the exponential behavior for short polymer chains is attributed to end group effects for N up to 400 [39]. The polymer length we studied here spans a much wider range, therefore the deviation from a single exponential decay might suggest that the separation parameter for dextran σ_d is not a constant, but is a function of N. In Fig. 9, we plotted the natural logarithm of the distribution coefficient of dextran, $-\ln(f_d(N))$, as a function of N_d. In the limit of long dextran chain with $N_d > 1500$, we observed a scaling relation of $-\ln(f_d(N)) \sim N_d^{\delta}$ with $\delta = 0.63$. This exponent has been reported earlier in the literature [13,14] for the distribution of polyethylene in diphenyl ether phase separated at several temperatures, and is still lacking theoretical interpretation. To account for the nonlinear exponential behavior, the degree of fractionation for dextran $f_d(N)$ was fitted by an empirical relation [39]

$$f_d(N) = A \times exp\left(-\sigma_d N - \sigma_{d2} N^{0.5}\right) \quad (3)$$

where two additional fitting parameters A and σ_{d2} are introduced. Fitting of the data to Eq. (3) is rather good (Fig. 8). Knowing the degree of fractionation for dextran $f_d(N)$ as a function of N_d, together with the weight fraction of each phase obtained by mass balance on the tie line, one can calculate the molar mass distribution of dextran in the two phases [19,27]. Fig. 6a shows the calculated molar mass distribution curves of dextran in the two phases at reduced polymer concentration $\varepsilon = 0.01$, which are in excellent agreement with the experimental results. As shown in Fig. 7a, the resulting weight average molar masses of dextran in both phases are in good agreement with the GPC results at all reduced polymer concentration ε between 0.01 and 0.73.

On the other hand, the molar mass distributions of PEG are both rather narrow and very similar in the two phases, which leads to essentially constant values of the degree of fractionation $f_p(N)$ over

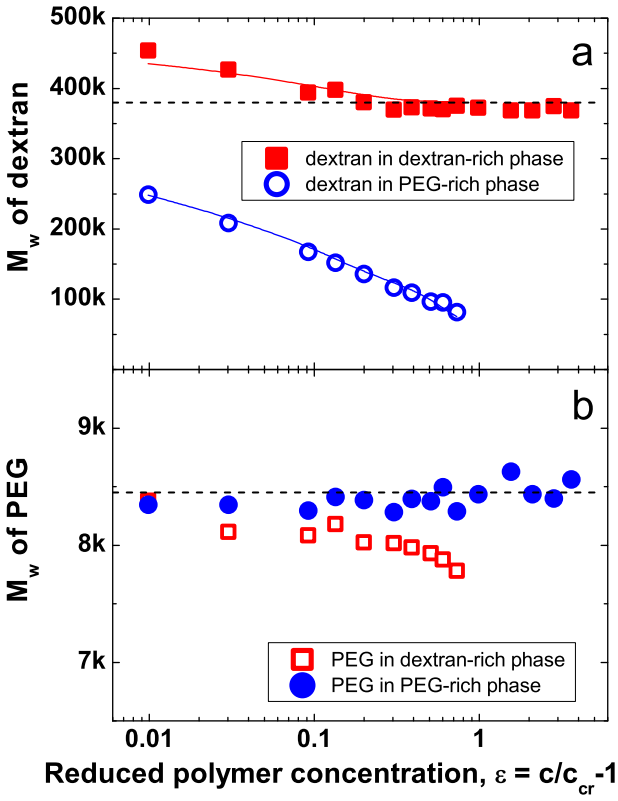

Fig. 7. Weight average molar mass M_w of dextran (a) and PEG (b) in dextran-rich (squares) and PEG-rich (circles) phases. The dashed lines indicate the average molar mass M_w = 380 kg/mol for dextran and M_w = 8.45 kg/mol for PEG, respectively. The M_w–values of dextran in the two phases, which were obtained from the calculated molar mass distribution of dextran, are shown as solid lines in panel (a).

the accessible range of N_p–values for all reduced polymer concentrations ε. Previous studies on ATPS with dextran and PEG, both with broad molar mass distribution, did observe the exponential decay behaviors of the degree of fractionation for both dextran and PEG between the coexisting phases [20].

Because the narrow molar mass distribution of PEG used in this study did not allow us to observe the exponential dependence

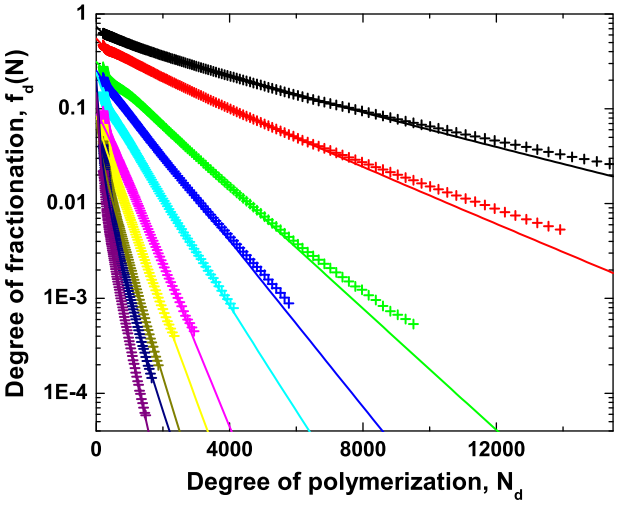

Fig. 8. Degree of fractionation $f_d(N)$ for dextran as a function of the degree of polymerization N_d of dextran for different values of the reduced polymer concentration ε which is varied from 0.01 (top right) to 0.73 (bottom left). The lines are fits to the data by the empirical relation in Eq. (3).

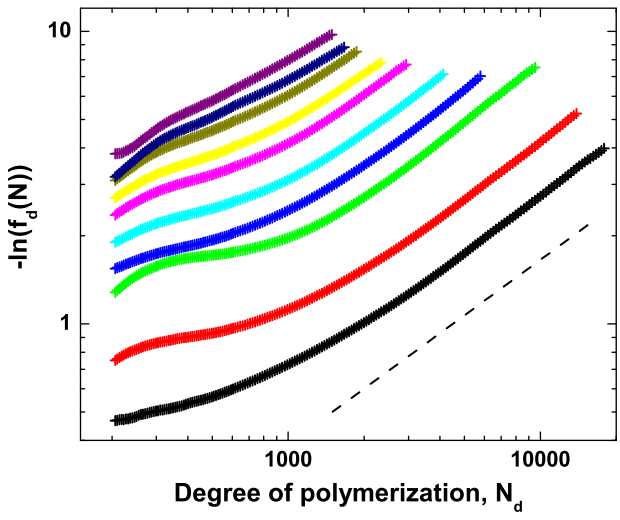

Fig. 9. The natural logarithm of the degree of fractionation for dextran, $-\ln(f_d(N))$, as a function of the degree of polymerization N_d of dextran for different values of the reduced polymer concentration ε which is varied from 0.01 (bottom) to 0.73 (top). The dashed line indicates a slope of 0.63.

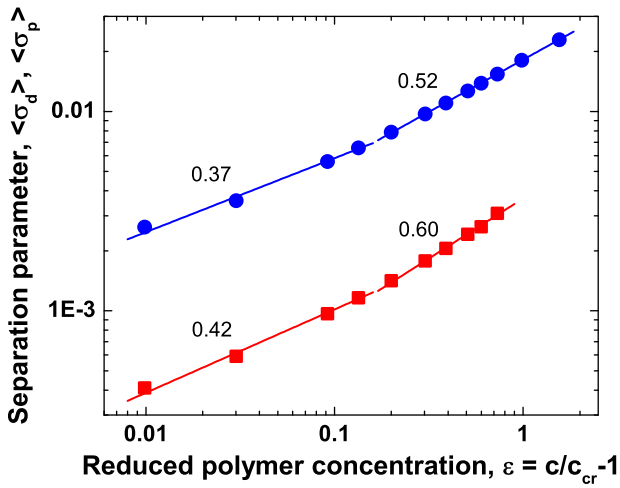

Fig. 10. Average separation parameters $\langle\sigma_d\rangle$ for dextran (solid squares), and $\langle\sigma_p\rangle$ for PEG (solid circles), as functions of reduced polymer concentration. In the concentration range $0.01 < \varepsilon < 0.14$, the data were well fitted by the effective scaling exponents 0.371 ± 0.024 for PEG and 0.418 ± 0.024 for dextran, while in the range $0.2 < \varepsilon < 1.5$, the fit leads to the exponent values 0.525 ± 0.002 for PEG and 0.603 ± 0.020 for dextran.

of $f_p(N)$ on chain length N_p, we considered an average separation parameter $\langle\sigma_p\rangle$ for the PEG chains as defined by

$$\langle\sigma_p\rangle = -ln\left(c_p^D/c_p^P\right)/\langle N_p\rangle \quad (4)$$

where $c_p{}^D$ and $c_p{}^P$ are total PEG concentrations in the dextran-rich and PEG-rich phases, respectively. The average PEG length $\langle N_p\rangle$ is 192 according to its M_w of 8450 g/mol.

Similarly, we defined an average separation parameter $\langle\sigma_d\rangle$ for dextran via

$$\langle\sigma_d\rangle = -ln\left(c_d^P/c_d^D\right)/\langle N_d\rangle \quad (5)$$

where $c_d{}^P$ and $c_d{}^D$ are total dextran concentrations in the PEG-rich and dextran-rich phases, respectively. The average dextran length $\langle N_d\rangle$ is 2345 with a monomer mass of 162 g/mol.

The average separation parameters of dextran and PEG are plotted in Fig. 10 as functions of reduced polymer concentration. The separation parameters σ_x scale with the reduced polymer concentration ε according to $\sigma_x \sim \varepsilon^{\beta'}$ where the effective scaling exponent

β' attains two distinct values within two concentration ranges: (i) in the concentration range $0.01 < \varepsilon < 0.14$ (regime I), the scaling exponent β' has the values 0.37 for PEG and 0.42 for dextran, and (ii) in the range $0.2 < \varepsilon < 1.5$ (regime II), this exponent has the values 0.52 for PEG and 0.60 for dextran. The values for PEG are close to the Ising value of $\beta = 0.326$ for regime I and the mean field value $\beta = 1/2$ for regime II, i.e., $\beta' \approx \beta$. Although the values for dextran are slightly high, due to the effect of polymer fractionation on the phase composition (discussed further below), one does observe a crossover of the exponent from a higher value to a lower one as moves closer to the critical point, corresponding to a crossover from mean field to Ising model behavior. In a previous study on polymer fractionation in ATPS based on computer simulations [39], the scaling exponent between the separation parameter and the reduced temperature took a value of 1/2, in accord with the mean field value of $\beta = 1/2$. We have shown here that non-mean-field behavior is expected as the critical point is approached.

Polymer fractionation during phase separation of dextran with a broad molar mass distribution and PEG with a narrow molar mass distribution leads to the redistribution of dextran of different chain lengths between the two phases. Long dextran chains are enriched in the dextran-rich phase, and depleted from the PEG-rich phase. These findings provide an explanation for the mismatch between the tie line end points of the PEG-rich phase close to the critical point and the binodal curve (see inset of Fig. 4). These tie line end points in the PEG-rich phase contain dextran with molar mass lower than the original dextran (Table 2), and therefore are shifted upwards in the phase diagram compared with the binodal. On the other hand, the tie line end points in the dextran-rich phase contain dextran of slightly higher molar mass (Table 2), and are expected to locate below the binodal, although the effect is too small to be observed. These observations are in excellent agreement with previous calculations based on the UNIQUAC model [18]. To determine the phase compositions of such ATPS system close to the critical point by the density method [11], one should first locate the composition of the dextran-rich phase, and then estimate the composition of the PEG-rich phase from the intersection of the isopycnic line with a line passing through the coordinates of the initial composition and the dextran-rich phase composition. In this way, the simple density method can be employed for the determination of the tie line end points for ATPS system containing dextran with a broad molar mass distribution and PEG with a narrow molar mass distribution.

The results also explain the discrepancy between the observed scaling exponent of 1.67 and the Ising model value 1.26 for the interfacial tension as a function of reduced polymer concentration [11]. Theory of the interfacial tension of immiscible polymer blends in solution indicates a strong molar mass dependence of the interfacial tension $\sigma \sim M^{-d}$ with $d \approx 1.10$ [40], as demonstrated by the two-phase system of polystyrene—poly(dimethylsiloxane) dissolved in toluene with polymer molar masses of 270 and 734 kg/mol, respectively [41]. For polymer compositions close to the critical point, dextran in the dextran-rich phases has an averaged molar mass larger than that of the original dextran, which reduces the interfacial tension and leads to a scaling exponent larger than the Ising model value of 1.26. For polymer compositions far away from the critical point, dextran in the dextran-rich phases has a molar mass very close to that of the original sample, the interfacial tension is unaffected and the mean field value of 3/2 is observed.

Our results show that mean-field theory is only applicable to ATPS with compositions sufficiently far away from the critical point. This should be kept in mind when modeling ATPS with Flory-Huggins theory. Studying the biomolecules partitioning in ATPS with well-characterized compositions and molar mass distributions of the coexisting phases will help to elucidate the underlying mechanisms of their partitioning.

4. Conclusions

Both composition and molar mass distribution of dextran and PEG in phase separated aqueous solutions of these two polymers were studied by GPC. The resulting tie lines by the GPC method confirm those established by the method based on density measurements of the phases. For solutions of dextran with a broad molar mass distribution and PEG with a narrow molar mass distribution, fractionation of dextran during phase separation of the aqueous mixtures was observed. The degree of fractionation $f_d(N)$ for dextran shows an exponential decay on the chain length N_d. The average separation parameters for both dextran and PEG show a crossover from Ising model to mean field behavior with increasing distance from the critical point. Long dextran chains are enriched in the dextran-rich phase and depleted from the PEG-rich phase, which leads to the observed deviation of the scaling exponent for the interfacial tension from the Ising model behavior close to the critical point.

Acknowledgements

We thank Helmut Schlaad for his help in part of the GPC experiments. This work is supported by the Partner Group Program of the Max Planck Society and the Chinese Academy of Sciences, the National Natural Science Foundation of China (21274147), the Natural Science Foundation of Jilin Province, China (201215093), and the China-South Africa Joint Research Program.

References

[1] P.Å. Albertsson, Partition of Cell Particles and Macromolecules: Separation and Purification of Biomolecules, Cell Organelles, Membranes, and Cells in Aqueous Polymer Two-Phase Systems and Their Use in Biochemical Analysis and Biotechnology, 3rd ed, Wiley, New York, 1986.
[2] H. Walter, D.E. Brooks, D. Fisher, Partitioning in Aqueous Two-phase Systems: Theory, Methods, Uses, and Applications to Biotechnology, Academic Press, Orlando, 1985.
[3] S. Hardt, T. Hahn, Microfluidics with aqueous two-phase systems, Lab Chip 12 (2012) 434–442.
[4] P.A.J. Rosa, I.F. Ferreira, A.M. Azevedo, M.R. Aires-Barros, Aqueous two-phase systems: a viable platform in the manufacturing of biopharmaceuticals, J. Chromatogr. A 1217 (2010) 2296–2305.
[5] A.D. Diamond, J.T. Hsu, Aqueous two-phase systems for biomolecule separation, Adv. Biochem. Eng./Biotechnol. 47 (1992) 89–135.
[6] H.-O. Johansson, G. Karlstrom, F. Tjerneld, C.A. Haynes, Driving force for phase separation and partitioning in aqueous two-phase systems, J. Chromatogr. B 711 (1998) 3–17.
[7] J.A. Asenjo, B.A. Andrews, Aqueous two-phase systems for protein separation: a perspective, J. Chromatogr. A 1218 (2011) 8826–8835.
[8] E. Atefi, R. Joshi, J.A. Mann, H. Tavana, Interfacial tension effect on cell partition in aqueous two-phase systems, ACS Appl. Mater. Interfaces 7 (2015) 21305–21314.
[9] R. Hatti-Kaul, Methods in biotechnology Aqueous Two-Phase Systems: Methods and Protocols, vol. 11, Humana Press, Totowa, 2000.
[10] J.C. Merchuk, B.A. Andrews, J.A. Asenjo, Aqueous two-phase systems for protein separation studies on phase inversion, J. Chromatogr. B 711 (1998) 285–293.
[11] Y. Liu, R. Lipowsky, R. Dimova, Concentration dependence of the interfacial tension for aqueous two-phase polymer solutions of dextran and polyethylene glycol, Langmuir 28 (2012) 3831–3839.
[12] R. Koningsveld, W.H. Stockmayer, J.W. Kennedy, L.A. Kleintjens, Liquid-liquid phase separation in multicomponent polymer systems. XI. Dilute and concentrated polymer solutions in equilibrium, Macromolecules 7 (1974) 73–79.
[13] L.A. Kleintjens, R. Koningsveld, W.H. Stockmayer, Liquid-liquid phase separation in multicomponent polymer systems XIV. Dilute and concentrated polymer solutions in equilibrium (continued), Br. Polym. J. 8 (1976) 144–151.
[14] R. Koningsveld, L.A. Kleintjens, H. Geerissen, P. Schutzeichel, B.A. Wolf, Fractionation, in: G. Allen (Ed.), Comprehensive Polymer Science, Pergamon Press, Oxford, 1989, pp. 293–312.
[15] G. ten Brinke, I. Szleifer, Liquid-liquid phase separation in polydisperse polymer solutions: the distribution coefficient, Macromolecules 28 (1995) 5434–5439.

[16] R.S. Shresth, R.C. McDonald, S.C. Greer, Molecular weight distributions of polydisperse polymers in coexisting liquid phases, J. Chem. Phys. 117 (2002) 9037–9049.
[17] R. Koningsveld, W.H. Stockmayer, E. Nies, Polymer Phase Diagrams, Oxford University Press, New York, 2001.
[18] C.H. Kang, S.I. Sandler, Effects of polydispersivity on the phase behavior of the aqueous two-phase polymer systems, Macromolecules 21 (1988) 3088–3095.
[19] M.W. Edelman, R.H. Tromp, E. van der Linden, Phase-separation-induced fractionation in molar mass in aqueous mixtures of gelatin and dextran, Phys. Rev. E 67 (2003) 021404.
[20] M.W. Edelman, E. van der Linden, R.H. Tromp, Phase separation of aqueous mixtures of poly(ethylene oxide) and dextran, Macromolecules 36 (2003) 7783–7790.
[21] M. Connemann, J. Gaube, U. Leffrang, S. Muller, A. Pfennig, Phase equilibria in the system poly(ethylene glycol) + dextran + water, J. Chem. Eng. Data 36 (1991) 446–448.
[22] Z. Zhao, Q. Li, Y. Xue, X. Ji, S. Bo, Y. Liu, Composition and molecular weight determination of aqueous two-phase system by quantitative size exclusion chromatography, Chem. J. Chin. Univ. 37 (2016) 167–173.
[23] B.Y. Zaslavsky, Aqueous Two-phase Partitioning Physical Chemistry and Bioanalytical Applications, Marcel Dekker, New York, 1994.
[24] H. Cabezas Jr., Theory of phase formation in aqueous two-phase systems, J. Chromatogr. B 680 (1996) 3–30.
[25] E. Edmond, A.G. Ogston, An approach to the study of phase separation in ternary aqueous systems, Biochem. J. 109 (1968) 569–576.
[26] T.L. Hill, Theory of solutions. II. Osmotic pressure viral expansion and light scattering in two component solutions, J. Chem. Phys. 30 (1959) 93–97.
[27] P.J. Flory, Principles of Polymer Chemistry, Cornell University Press, Ithaca, 1953.
[28] C.H. Kang, S.I. Sandler, A thermodynamic model for two-phase aqueous polymer systems, Biotech. Bioeng. 32 (1988) 1158–1164.
[29] Y. Guan, T.H. Lilley, T.E. Treffry, A new excluded volume theory and its application to the coexistence curves of aqueous polymer two-phase systems, Macromolecules 26 (1993) 3971–3979.
[30] B.Y. Zaslavsky, T.O. Bagirov, A.A. Borovskaya, N.D. Gulaeva, L.H. Miheeva, A.U. Mahmudov, M.N. Rodnikova, Structure of water as a key factor of phase separation in aqueous mixtures of two nonionic polymers, Polymer 30 (1989) 2104–2111.
[31] A.D. Diamond, J.T. Hsu, Protein partitioning in PEG/dextran aqueous two-phase systems, AIChE J. 36 (1990) 1017–1023.
[32] N.L. Abbott, D. Blankschtein, T.A. Hatton, Protein partitioning in two-phase aqueous polymer systems. 1. Novel physical pictures and a scaling-thermodynamic formulation, Macromolecules 24 (1991) 4334–4348.
[33] P.P. Madeira, C.A. Reis, A.E. Rodrigues, L.M. Mikheeva, A. Chait, B.Y. Zaslavsky, Solvent properties governing protein partitioning in polymer/polymer aqueous two-phase systems, J. Chromatogr. A 1218 (2011) 1379–1384.
[34] P.P. Madeira, A. Bessa, L. Alvares-Ribeiro, M.R. Aires-Barros, C.A. Reis, A.E. Rodrigues, B.Y. Zaslavsky, Salt effects on solvent features of coexisting phases in aqueous polymer/polymer two-phase systems, J. Chromatogr. A 1229 (2012) 38–47.
[35] F.E. Bailey, J.L. Kucera, L.G. Imhof, Molecular weight relations of poly(ethylene oxide), J. Polym. Sci. 32 (1958) 517–518.
[36] F.R. Senti, N.N. Hellman, N.H. Ludwig, G.E. Babcock, R. Tobin, C.A. Glass, B.L. Lamberts, Viscosity sedimentation, and light-scattering properties of fraction of an acid-hydrolyzed dextran, J. Polym. Sci. 17 (1955) 527–546.
[37] C.E. Ioan, T. Aberle, W. Burchard, Structure properties of dextran. 2. dilute solution, Macromolecules 33 (2000) 5730–5739.
[38] M.R. Helfrich, L.K. Mangeney-Slavin, M.S. Long, Y. Djoko, C.D. Keating, Aqueous phase separation in giant vesicles, J. Am. Chem. Soc. 124 (2002) 13374–13375.
[39] A. van Heukelum, G.T. Barkema, M.W. Edelman, E. van der Linden, E.H.A. de Hoog, R.H. Tromp, Fractionation in a phase-separated polydisperse polymer mixture, Macromolecules 36 (2003) 6662–6667.
[40] D. Broseta, L. Leibler, J.-F. Joanny, Critical properties of incompatible polymer blends dissolved in a good solvent, Macromolecules 20 (1987) 1935–1943.
[41] D. Broseta, L. Leibler, L.O. Kaddour, C. Strazielle, A theoretical and experimental study of interfacial tension of immiscible polymer blends in solution, J. Chem. Phys. 87 (1987) 7248–7256.